

Angular, Temperature, and Strain Dependencies of the Critical Current of DI-BSCCO Tapes in High Magnetic Fields

Prapaiwan Sunwong, Joshua S. Higgins, and Damian P. Hampshire

Abstract—High critical current density (J_c) DI-BSCCO Bi-2223 superconducting tape has been developed by Sumitomo Electric Industries (SEI) using the Controlled Over-Pressure (CT-OP) technique to improve the texturing and densification. Further enhancement of the mechanical properties has been obtained using lamination. We have investigated the effect of magnetic field and field orientation on J_c for a series of test DI-BSCCO tapes at 77 K and 4.2 K under tensile and compressive strains. These critical current data are strongly influenced by the anisotropy of Bi-2223, the texturing of the tape and its architecture. The magnetic field and angular dependence of J_c at 77 K can be described using a simple anisotropic exponential magnetic field model which includes the effects of the two-dimensionality and grain misalignment in these composites. The variation in the normalized J_c with respect to the strain is linear over the reversible range of strain where the gradient of the strain dependence is independent of temperature and field. The reversibility of J_c is extended further into the compressive regime after J_c degradation by compression.

Index Terms—Angular dependence, BSCCO, critical current, reversible strain limit.

I. INTRODUCTION

THE CONTROLLED Over-Pressure (CT-OP) technique is used by SEI to improve the texturing and densification of DI-BSCCO Bi-2223 multifilament superconducting tapes produced by the Powder-in-tube method [1]–[3]. CT-OP DI-BSCCO tape has high J_c in high magnetic fields and excellent mechanical strength. It is valuable for many applications such as power cables, transformers, motors, generators and high field magnets. The performance of these tapes under the strains that they will experience when they are used is an important issue. Further enhancement of the mechanical properties has been obtained by including laminations which leads to an increase in thermally induced compressive residual strain exerted on the superconducting components and hence a reversible tensile strain limit [4], [5].

A significant feature of high temperature superconducting (HTS) tape is the anisotropy which plays a critical

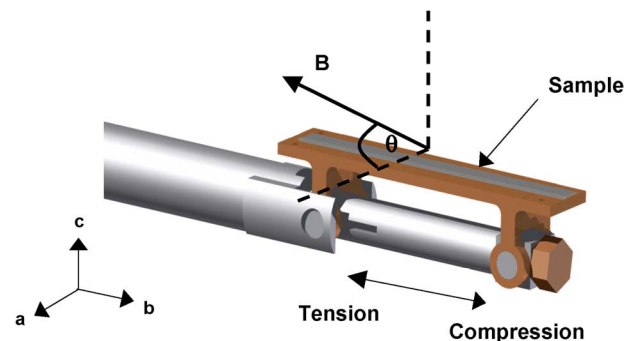


Fig. 1. Experimental apparatus for the strain measurements.

role in the current transport and mechanical properties. Several models have been introduced to describe the percolative local current path [6], [7] and the magnetic field and angular dependence of J_c [8], [9]. A comprehensive and deep understanding of these materials will be necessary to assess the technological potential of these materials and to use their unique properties successfully in applications. In this work, we investigate the effect of magnetic field and field orientation on the J_c of a series of DI-BSCCO test sample tapes at 77 K and 4.2 K under tensile and compressive strain.

II. EXPERIMENTAL METHOD

The CT-OP processed test sample DI-BSCCO tapes were provided by SEI. The J_c measurements were carried out using a standard four-terminal technique and the critical currents were determined using a $100 \mu\text{Vm}^{-1}$ electric field criterion. All critical current densities in this work are calculated using the critical current divided by the unstrained cross-sectional area of the superconducting filaments. The measurements were performed at 77 K in a conventional iron-cored electromagnet in magnetic fields up to 0.7 T and at 4.2 K in the 15 T horizontal superconducting split-pair magnet at different angles (θ) between the field and the tape surface. In the strain measurements, the DI-BSCCO tapes were mounted on a springboard-shaped copper beryllium sample holder, which is attached at one end to a moveable inner stainless steel tube and has the other end supported by an outer tube. The compressive and tensile strains were applied to the tapes by pushing or pulling the inner tube. The strain was measured with a Vishay strain gauge attached onto the surface of sample holder next to the sample. A schematic of the experimental apparatus for the strain measurements is shown in Fig. 1. An HGCT-3020 Hall sensor from Lake Shore Cryogenic, Inc. was used to investigate whether

Manuscript received August 03, 2010; accepted November 29, 2010. Date of publication January 10, 2011; date of current version May 27, 2011. This work was supported by Sumitomo Electric Industries, Ltd., Konohana-ki, Osaka 554-0024, Japan.

The authors are with the Department of Physics, Centre for Materials Physics, Durham University, Durham DH1 3LE, U.K. (e-mail: prapaiwan.sunwong@durham.ac.uk).

Color versions of one or more of the figures in this paper are available online at <http://ieeexplore.ieee.org>.

Digital Object Identifier 10.1109/TASC.2010.2097573

TABLE I
 TEST SAMPLES OF DI-BSCCO TAPES

Sample	Type	Average width (mm)	Average thickness (mm)	Lamination	
				Material	Thickness (μm)
1. Bare	H	4.3 ± 0.3	0.23 ± 0.03	-	-
2. SS20	HT	4.5 ± 0.3	0.30 ± 0.04	SUS	20
3. Ag20	HT	4.5 ± 0.3	0.30 ± 0.04	Cu-Ag alloy	20
4. CA50	HT	4.5 ± 0.3	0.36 ± 0.04	Cu alloy	50

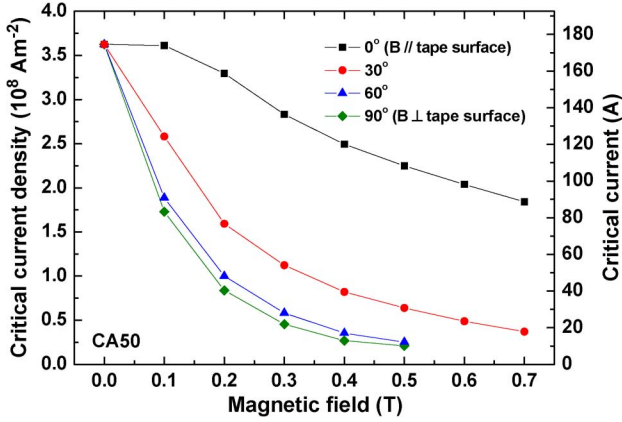


Fig. 2. Critical current density as a function of the applied magnetic field for the DI-BSCCO CA50 tape at 77 K for different field orientations.

the sample rotated during the J_c measurement while the top of the probe was fixed. The sensor was attached directly on to the sample and the component of the magnetic field orthogonal to the surface of the Hall sensor was continuously monitored. The sensor has the maximum linearity error $\pm 1.0\%$ for fields less than 3 T and $\pm 2.0\%$ for fields up to 15 T. A general description and the specifications of the four DI-BSCCO tapes used in this study are summarized in Table I.

III. RESULTS AND DISCUSSION

A. Magnetic Field and Angular Dependencies of the Critical Current Density

The anisotropic properties of DI-BSCCO tape are shown in Fig. 2 and Fig. 3 for the CA50 tape. The results from the other three samples are similar. Fig. 2 shows J_c as a function of the applied magnetic field for different angles between the field and the tape surface. J_c is higher when the field is parallel to the tape surface than when the field is normal to the surface because of the intrinsic pinning associated with the Cu-O planes and the higher upper critical field [10], [11]. Fig. 3 gives J_c as a function of the angle between the field and the tape surface and clearly shows the intrinsic peaks. Our current understanding of the field dependence of J_c is that because of the strongly two-dimensional nature of BSCCO, the local component of the field along the c -axis determines the in-field decrease of J_c [12]. Fig. 4 shows the J_c of the DI-BSCCO CA50 tape as a function of this field component. The data for the field applied perpendicular to the tape surface are made more explicit for clarity. $J_c(B \sin \theta)$ coincides with the data set for $J_c(B \text{ normal to the surface})$ in

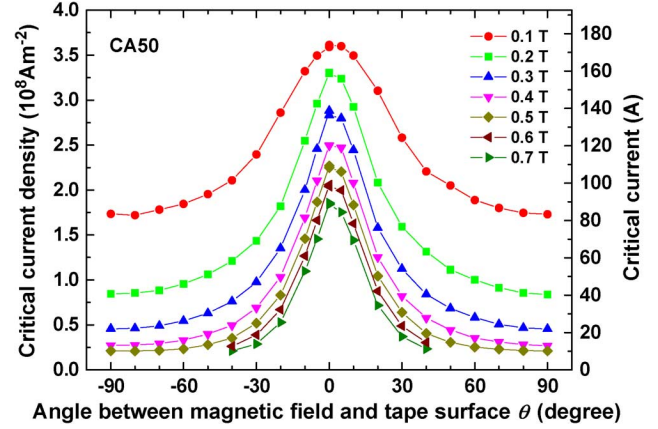
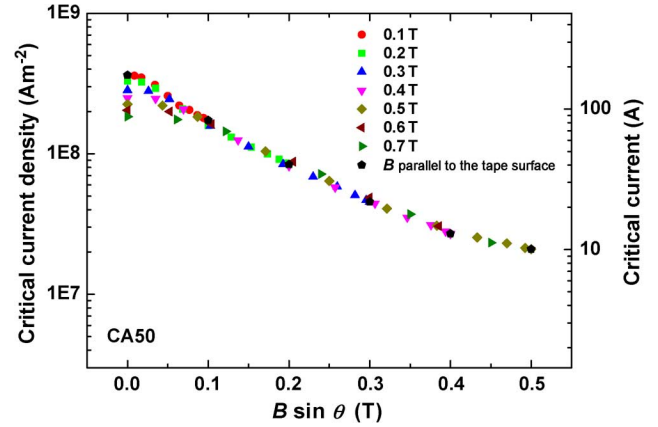


Fig. 3. Critical current density as a function of the angle between the applied magnetic field and the surface of the DI-BSCCO CA50 tape at 77 K at different applied magnetic fields.


 Fig. 4. Critical current density as a function of the magnetic field component normal to the tape surface ($B \sin \theta$) of the DI-BSCCO CA50 tape at 77 K.

the high field region but deviates in the low field region consistent with misalignment of the grains within the tapes [13], [14].

The work of Meer *et al.* considers a Gaussian distribution function to describe grain misalignment with a standard deviation σ , given by an equation of the form [13]

$$G(\varphi) = \frac{1}{\sigma\sqrt{2\pi}} \exp\left(\frac{-\varphi^2}{2\sigma^2}\right) \quad (1)$$

This distribution accounts for a small angle between the field and the local ab-plane of the grains within the tape where $G(\varphi)d\varphi$ is the fraction of grains that have a misalignment angle between φ and $d\varphi$ where $-90^\circ \leq \varphi < 90^\circ$. If a magnetic field is applied at an angle θ with respect to the tape surface and the grains locally have a misalignment angle φ , the local orientation of the magnetic field with respect to the ab-plane becomes $\theta + \varphi$. As a result, the local magnetic field parallel to the c -axis is $B \sin(\theta + \varphi)$. The average effective magnetic field orthogonal to the tape surface is:

$$B_{eff}(\theta) = B \int_{-90^\circ}^{90^\circ} G(\varphi) |\sin(\theta + \varphi)| d\varphi \quad (2)$$

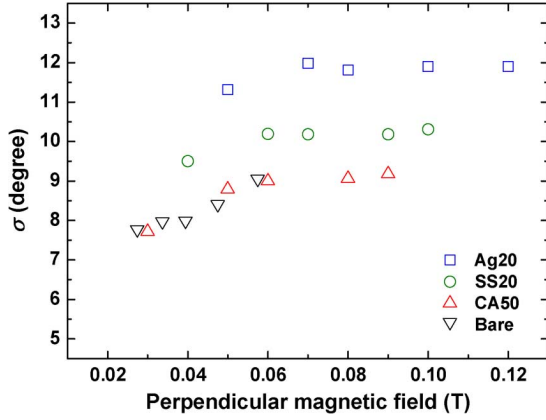


Fig. 5. Standard deviation of misalignment angle as a function of magnetic field normal to the tape surface for the different types of the DI-BSCCO tapes.

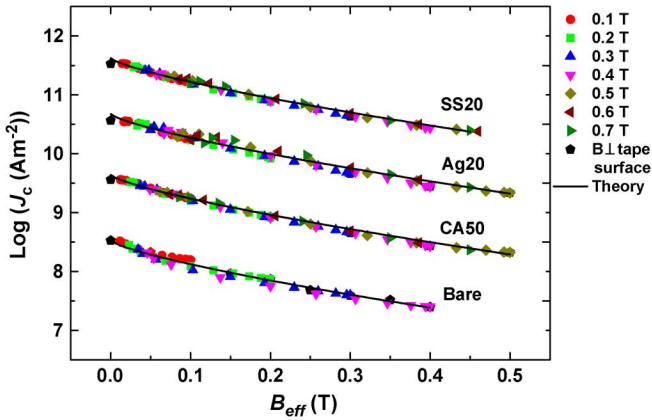


Fig. 6. Critical current density as a function of the effective magnetic field for the DI-BSCCO tapes at 77 K. The data for each tape are increased sequentially by 1 from the bare tape for clarity.

A scaling function $f(\theta)$ introduced by Shevchenko [15] is introduced by normalizing $B_{eff}(\theta)$ with respect to $B_{eff}(90^\circ)$ which is independent on the magnitude of the magnetic field but depends on the field orientation. For any magnetic field applied at an angle θ with respect to the tape surface, the scaled field amplitude of the effective perpendicular magnetic field is written as $B \times f(\theta)$. The value of $f(0^\circ)$ can be determined from the experimental results where J_c is a function of the magnetic field at the angles 0° and 90° and using the relation $J_c(B, 0^\circ) = J_c(B \times f(0^\circ), 90^\circ)$. The value of σ is calculated using:

$$\sigma = 70.9f(0^\circ) \quad (3)$$

which is accurate to 1% where σ represents the standard deviation in the grain misalignments within the tape and is in principle not dependent on the magnetic field [13]. Fig. 5 shows the calculated values of σ for the four different types of the DI-BSCCO tape measured. The scaling function $f(\theta)$ for any given θ is then obtained using the calculated value of σ from (3), which is 12° for the Ag20 tape, 10° for the SS20 tape, 9° for the CA50 tape and 9° for the bare tape.

Fig. 6 shows J_c for the DI-BSCCO tapes as a function of the effective field $B \times f(\theta)$ at 77 K; the $\log(J_c)$ data of CA50, Ag20 and SS20 tapes are increased sequentially by 1 from the bare

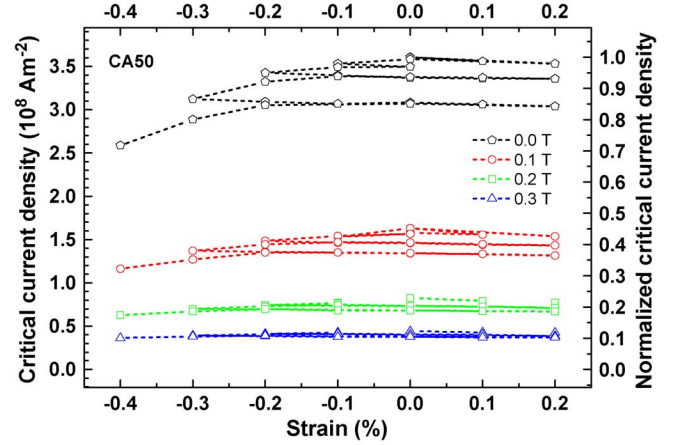


Fig. 7. Critical current density as a function of strain of the DI-BSCCO CA50 tape at 77 K for different fields parallel to the c-axis. The normalization constant is 173.7 Amps.

tape for clarity. The deviation, associated with the misalignment of grains seen in Fig. 4 in the low field region has disappeared. We propose that the J_c can be described using the model derived for granular superconductors [16]:

$$J_c(B, T, \theta) = \alpha(T) \left(1 - \frac{B_{eff}(\theta)}{B_{c2}(T, \varepsilon = 0, \theta = 90^\circ)} \right) \times \exp \left[- \left(\frac{B_{eff}(\theta)}{\beta(T, \varepsilon = 0)} \right)^m \right] \quad (4)$$

where we have added the parameter m to account for the non-exponential behavior at low fields and the term $B_{c2}(T, \varepsilon = 0, \theta = 90^\circ)$ is the upper critical field when the magnetic field is applied normal to the tape surface. α is a parameter representing the depairing current density; β characterizes the suppression of the order parameter by the magnetic field across grain boundaries and is found experimentally not to depend on angle or strain (cf below). Equation (4) accounts for the reduction in the depairing current density due to the depression of the order parameter by the magnetic field at the grain boundaries and the suppression of the order parameter within the grains themselves [16]. Solid lines in Fig. 6 are plots of (4) using the parameters $\beta = 0.11$ T and $m = 0.75$. α varies from sample to sample and is 4.2×10^8 for the SS20 tape, 4.7×10^8 for the Ag20 tape, 4.4×10^8 for the CA50 tape and 3.4×10^8 for the bare tape. The value of B_{c2} was found to be much higher than B_{eff} . Hence the suppression of the order parameter within the grains can be considered negligible.

B. Strain Dependence of the Critical Current Density

The variation in the J_c caused by the tensile and compressive strain is shown in Fig. 7 for the DI-BSCCO CA50 tape at 77 K at different magnetic fields applied perpendicular to the tape surface. The J_c -strain characteristics for different fields are similar. The strain was initially applied in tension causing the J_c to reduce reversibly. This behavior in Bi-2223 superconducting tapes in zero field at 77 K has been reported earlier by others [4], [5], [17]. We investigated the bare tape (not shown here) and the laminated CA50 tape. The lamination produces higher reversible strain limits and suppresses irreversible

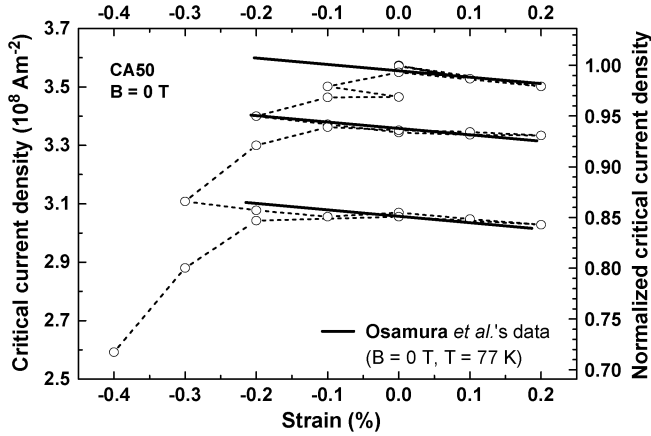


Fig. 8. Critical current density as a function of strain of the DI-BSCCO CA50 tape at 77 K for zero field. The solid lines are taken from Osamura *et al.*'s data at 77 K in self-field [4]. The normalization constant is 173.7 Amps.

behavior. The improvements are due to increased compressive residual strain exerted on the filaments due to the difference in the coefficients of thermal expansion of various components of the laminated composites.

Fig. 8 shows the variable strain dependence of J_c for the DI-BSCCO CA50 tape at 77 K for zero field alone. Fig. 9 shows variable data at 4.2 K and $B = 10$ T. Both data sets show similar behavior namely that initially although J_c is reversible in tension, there is no reversibility in compression. On applying increased compression there is an irreversible degradation. Thereafter on reducing the compressive strain one finds an increased reversible range stretching over both tensile and compressive strains. Figs. 8 and 9 each show three different reversible ranges. We note that reversibility in tension still occurs after degradation of J_c and that the reversibility is extended into the compressive regime. In the reversible strain regime the variation in the normalized J_c with respect to the strain is linear, both at 77 K and 4.2 K and can be described by:

$$J_c(B, T, \theta, \varepsilon) = (1 - A\varepsilon) \times J_c(B, T, \theta) \quad (5)$$

where ε is the applied strain (%) and A is equal to 7.5×10^{-2} , independent on the temperature and magnetic field. Osamura *et al.*'s data at 77 K and zero field [4] are more detailed and show that A is a weak function of strain. Nevertheless, to first order, the value of A is similar and is shown in the figure by the solid lines. The most simple consistency between (4) and (5) leads to:

$$J_c(B, T, \theta, \varepsilon) = (1 - A\varepsilon)\alpha(T) \left(1 - \frac{B_{eff}(\theta)}{B_{c2}(T, \varepsilon = 0, \theta = 90^\circ)} \right) \times \exp \left[- \left(\frac{B_{eff}(\theta)}{\beta(T, \varepsilon = 0)} \right)^m \right] \quad (6)$$

Usually the changes in critical current caused by strain that are associated with geometrical changes are ignored because they are much smaller than the effect of strain on the superconducting parameters. We have observed a strain dependence for the critical current that has a functional form that resembles a strong geometrical factor with a gauge parameter A . This suggests that

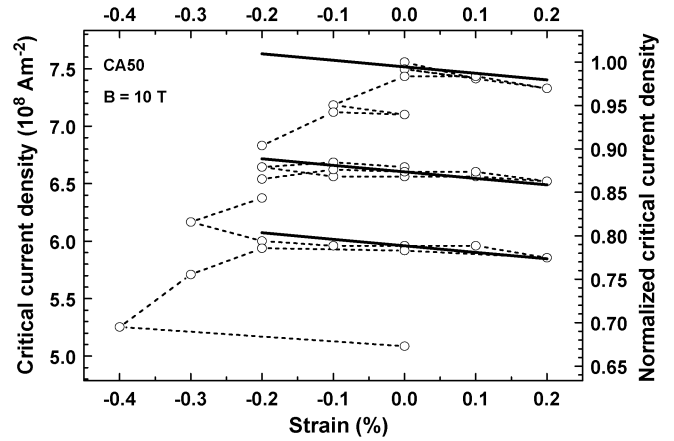


Fig. 9. Critical current density as a function of strain for the DI-BSCCO CA50 tape at $T = 4.2$ K and $B = 10$ T applied parallel to the c -axis. The solid lines have constant gradient. The normalization constant is 364.0 Amps.

at fields and temperatures well below B_{c2} and T_c , one can ignore their strain dependence or probably more strictly their functional form combines in a way that to first order leads to the gauge parameter behavior.

The irreversibility of J_c under compression for BSCCO tapes has been observed before [18]–[20]. A natural concern is whether this behavior is intrinsic for example associated with the strongly two-dimensionality of BSCCO leading to filament buckling or intragranular cracking under strain. This seems unlikely since the elastic constants and limits of BSCCO are only about a factor of 2–3 different from low temperature superconductors (LTS, e.g. Nb_3Sn). Certainly the (high) porosity of standard BSCCO conductors can lead to internal cracks and once the mechanical integrity of the composite is compromised, one can expect the full panoply of further damage including cracking and separation (or delamination) of the filaments from the matrix in both tension and compression [21], [22]. These world-class CP-OT BSCCO composites have very low porosity but still show irreversible behavior for J_c at relatively small compressive strains compared to LTS materials. Given the low Poisson ratio for BSCCO compared to metals and the difficulty of achieving strong bonding between metals and oxides, we suggest that the irreversible behavior J_c in these materials for small compression but not tension, may be explained by separation between the matrix and the filaments under compression. Given the non-uniform (sausaged) nature of the filaments, irreversibility need not necessarily be associated with damaged filaments rather initially it may be due to changes in interfilamentary current flow. Further study is needed to clarify the mechanism.

IV. CONCLUSION

The variation in the normalized J_c with respect to the strain is linear over the reversible range of strain with a gradient for the normalized J_c of $\sim 7.5 \times 10^{-2}$, independent of the magnetic field and temperature. In addition, the reversibility of J_c is extended further into the compressive regime after some irreversible behavior under strain.

ACKNOWLEDGMENT

The authors thank Prof. K. Osamura (RIAS) and Drs. K. Sato and J. Fujikami at SEI Ltd.

REFERENCES

- [1] M. Kikuchi *et al.*, "Development of new types of DI-BSCCO wire," *Sei Technical Review*, pp. 73–80, 2008.
- [2] M. Kikuchi *et al.*, "Recent development of drastically innovative BSCCO wire (DI-BSCCO)," *Physica C*, vol. 445–448, pp. 717–721, 2006.
- [3] N. Ayai *et al.*, "DI-BSCCO Wire with I_c over 200 A at 77 K," *Journal of Physics: Conference Series*, vol. 97, 2008.
- [4] K. Osamura *et al.*, "Improvement of reversible strain limit for critical current of DI-BSCCO due to lamination technique," *IEEE Trans. Applied Superconductivity*, vol. 19, pp. 3026–3029, 2009.
- [5] K. Osamura *et al.*, "Mechanical behavior and strain dependence of the critical current of DI-BSCCO tapes," *Superconductor Science & Technology*, vol. 21, 2008.
- [6] L. N. Bulaevskii *et al.*, "Model for the low-temperature transport of Bi-based high-temperature superconducting tapes," *Physical Review B*, vol. 45, pp. 2545–2548, 1992.
- [7] B. Hensel *et al.*, "A model for the critical current in $(\text{Bi,Pb})_2\text{Sr}_2\text{Ca}_2\text{Cu}_3\text{O}_x$ silver-sheathed tapes," *Physica C*, vol. 205, pp. 329–337, 1993.
- [8] G. M. Zhang *et al.*, "A theoretical model for the angular dependence of the critical current of BSCCO/Ag tapes," *Physica C*, vol. 390, pp. 321–324, 2003.
- [9] Y. Wang *et al.*, "Angular and magnetic field dependence of the critical current density of multifilamentary Bi2223 tapes," *Superconductor Science & Technology*, vol. 17, pp. 705–709, 2004.
- [10] J. R. Clem, "Two-dimensional vortices in a stack of thin superconducting films: A model for high-temperature superconducting multilayers," *Physical Review B*, vol. 43, pp. 7837–7846, 1991.
- [11] J. R. Clem, "Pancake vortices," *Journal of Superconductivity*, vol. 17, pp. 613–629, 2004.
- [12] P. Schmitt *et al.*, "Two-dimensional behavior and critical-current anisotropy in epitaxial $\text{Bi}_2\text{Sr}_2\text{CaCu}_2\text{O}_{8+x}$ thin films," *Physical Review Letters*, vol. 67, pp. 267–270, 1991.
- [13] O. van der Meer *et al.*, "A model to describe the angular dependence of the critical current in a Bi-2223/Ag superconducting tape," *Physica C*, vol. 357–360, pp. 1174–1177, 2001.
- [14] B. Xu *et al.*, "Dependence of transport critical current of magnetic field processed $\text{Bi}_2\text{Sr}_2\text{CaCu}_2\text{O}_8/\text{AgMg}$ tapes on the background magnetic field and magnetic field direction," *Superconductor Science & Technology*, vol. 18, pp. 503–507, 2005.
- [15] O. A. Shevchenko *et al.*, "AC loss in a high-temperature superconducting coil," *Physica C*, vol. 310, pp. 106–110, 1998.
- [16] D. P. Hampshire, "A barrier to increasing the critical current density of bulk untextured polycrystalline superconductors in high magnetic fields," *Physica C*, vol. 296, pp. 153–166, 1998.
- [17] H. J. N. van Eck *et al.*, "Bending and axial strain dependence of the critical current in superconducting BSCCO tapes," *Superconductor Science & Technology*, vol. 15, pp. 1213–1215, 2002.
- [18] B. ten Haken, A. Beuink, and H. H. J. ten Kate, "Small and repetitive axial strain reducing the critical current in BSCCO/Ag superconductors," *IEEE Trans. Applied Superconductivity*, vol. 7, pp. 2034–2037, 1997.
- [19] H. J. N. van Eck, L. Vargas, B. ten Haken, and H. H. J. ten Kate, "Bending and axial strain dependence of the critical current in superconducting BSCCO tapes," *Superconductor Science & Technology*, vol. 15, pp. 1213–1215, 2002.
- [20] Y. K. Huang, B. ten Haken, and H. H. J. ten Kate, "Strain and grain connectivity in Bi2223/Ag superconducting tapes," *IEEE Trans. Applied Superconductivity*, vol. 9, pp. 2702–2705, 1999.
- [21] J. Y. Pastor, P. Poza, and J. LLorca, "Mechanical properties of textured $\text{Bi}_2\text{Sr}_2\text{CaCu}_2\text{O}_{8+\delta}$ high-temperature superconductors," *Journal of the American Ceramic Society*, vol. 82, pp. 3139–3144, 1999.
- [22] A. Salazar, J. Y. Pastor, and J. LLorca, "Fatigue behavior of multifilamentary BSCCO 2223/Ag superconducting tapes," *IEEE Trans. Applied Superconductivity*, vol. 14, pp. 1841–1847, 2004.